

# Theoretical approach to ferroelectricity in hafnia and related materials

Hugo Aramberri<sup>1</sup> and Jorge Íñiguez<sup>1,2</sup>

<sup>1</sup>Materials Research and Technology Department, Luxembourg Institute of Science and Technology (LIST), Avenue des Hauts-Fourneaux 5, L-4362 Esch/Alzette, Luxembourg

<sup>2</sup>Department of Physics and Materials Science, University of Luxembourg, Rue du Brill 41, L-4422 Belvaux, Luxembourg

Hafnia ferroelectrics combine technological promise and unprecedented physical behaviors. Their peculiarity stems from the many active extrinsic mechanisms that contribute to their properties and from a continuously growing number of novel intrinsic features. Partly because of their unconventional nature, basic questions about these materials remain open, and there are inconsistencies between common theoretical assumptions and experimental evidence. Aided by first-principles simulations, here we show that many of hafnia's puzzles can be resolved by adopting an original high-symmetry reference phase as the starting point of the analysis. The proposed theory describes hafnia as a proper uniaxial ferroelectric that is not ferroelastic, correcting previous discrepancies with experiment while confirming key observations, such as the weak tendency of ferroelectric domains to grow. Our approach also provides a straightforward and unified description of all low-energy polymorphs, shedding light into old questions (e.g., the prevalence of the monoclinic ground state), pointing at exciting possibilities (e.g., an antiferroelastic behavior) and facilitating the future development of perturbative theories (from Landau to second-principles potentials). Our work thus yields a consistent and deeper understanding of hafnia ferroelectrics, improving our ability to optimize their properties and induce new ones.

Hafnia ferroelectrics [1, 2] – including  $\text{HfO}_2$ ,  $\text{Hf}_{1-x}\text{Zr}_x\text{O}_2$ ,  $\text{ZrO}_2$  and doped variations – attract attention because of their technological promise [3] and surprising properties, from their resilient polar order in nanostructures [1] to their tunable piezoresponse [4]. Understanding their behavior is challenging, though, a major difficulty coming from the variety of intrinsic and extrinsic factors that influence the observed properties. Even if we focus on the intrinsic features of perfect crystals, as those considered in quantum computer simulations, these materials prove exceedingly intriguing.

Here we argue that, in fact, in the case of the most common ferroelectric phase of hafnia (orthorhombic with space group  $Pca2_1$ ), we have not resolved yet an essential prerequisite to discuss ferroelectricity: what should be the centrosymmetric state used as a high-symmetry paraelectric reference. We contend that the common choices [5, 6] (well-known tetragonal and cubic polymorphs with

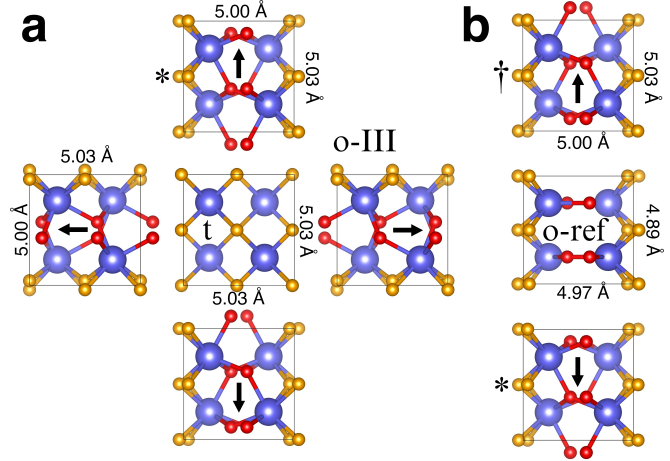


FIG. 1: **Ferroelectric domains expected in hafnia.** **a** shows the tetragonal (t) phase of hafnia (center) and the four orthorhombic ferroelectric (o-III) variants it leads to. **b** shows the orthorhombic centrosymmetric phase (o-ref) we propose as reference (center) and the two o-III domains it leads to. The active oxygens, responsible for the development of the spontaneous polarization, are shown in red; the other oxygens are shown in orange. Black arrows indicate the spontaneous polarization, which goes against the displacement of the active oxygens from the reference structure. The computed polarization with respect to the t-phase for the structure marked with an asterisk in **a** is  $+0.54 \text{ C m}^{-2}$ ; by contrast, the polarization with respect to the o-ref phase of the structure marked with a dagger presents  $+0.68 \text{ C m}^{-2}$ . (As shown in Supplementary Note 1,  $+0.54 \text{ C m}^{-2}$  and  $-0.68 \text{ C m}^{-2}$  differ by two polarization quanta.) Lattice constants are indicated; the strain that accompanies the polarization may yield ferroelastic domains in **a**, but not in **b**.

$P4_2/nmc$  and  $Fm\bar{3}m$  symmetries, respectively) do not suit key experimental observations. Then, based on first-principles simulations, we show that there exists an alternative reference that solves these issues while yielding an appealing model of ferroelectricity and related effects.

Let us first discuss the problems with current theories. Figure 1a sketches the most frequently considered paraelectric  $P4_2/nmc$  state (“t” in the following), and the variants of the  $Pca2_1$  ferroelectric phase (“o-III” in the following) obtained from this t-reference. The distortion from t to o-III breaks the tetragonal 4-fold axis, and the resulting polarization that can adopt four symmetry-equivalent orientations within the plane of the figure,  $(\pm P, 0)$  and  $(0, \pm P)$ . Accordingly, we expect to find

four different domains in hafnia samples; for example, we should observe ferroelectric and ferroelastic domain walls separating regions with  $\mathbf{P} = (P, 0)$  and  $\mathbf{P} = (0, P)$ . However, except for a recent report on an exotic charged ferroelectric (and ferroelastic) wall [7], such situations have not been observed as far as we know. In experiments hafnia appears to be a uniaxial ferroelectric that is not ferroelastic, which suggests that the t-phase is not a good choice of reference. (The problems get worse if a cubic reference is used.)

This reminds us of the ferroelectric  $R3c$  phase of  $\text{LiNbO}_3$  or LNO [8]. LNO shares symmetry and structural features with well-known ferroelectric perovskite  $\text{BiFeO}_3$  [9]; hence, it is tempting to treat LNO by choosing the prototype cubic perovskite lattice as paraelectric reference. That choice would imply that LNO's polarization can lie along eight symmetry-equivalent  $\langle 111 \rangle$  pseudo-cubic directions, yielding complex domain patterns as those observed in  $\text{BiFeO}_3$ . However, experiments show that LNO behaves as a uniaxial ferroelectric, suggesting that the cubic perovskite structure is not a suitable reference. Instead, a centrosymmetric  $R3c$  phase is the paraelectric state of LNO [10]. The distortion from  $R3c$  to  $R3c$  preserves the 3-fold axis and yields only two polarization variants, as corresponds to a uniaxial ferroelectric. These variants have the exact same strain, in agreement with the absence of ferroelasticity in LNO. In the case of the o-III phase of hafnia, we still need to find such a paraelectric reference compatible with experiments.

An additional issue pertains to the nature of ferroelectricity. Figure 2a shows the energy of hafnia computed along a path connecting t and o-III. (See Methods for calculation details.) Both structures are local energy minima, separated by a relatively high barrier, suggesting that a transition between them should be strongly discontinuous. Further, if the energy landscape is analyzed in terms of symmetry-adapted modes [6], one concludes that the o-III state displays an improper ferroelectric behavior, whereby the spontaneous polarization relies on the occurrence of several non-polar modes. This picture is appealing, because hafnia has been known to exhibit features typical of improper ferroelectrics (e.g., large coercive fields and, until recently, no clear sign of polar soft modes). However, fresh experiments question this interpretation.

Schroeder *et al.* [11] have recently reported a strong dielectric anomaly ( $\epsilon_r \approx 8000$ ) upon heating  $\text{Hf}_{0.5}\text{Zr}_{0.5}\text{O}_2$  across what seems to be a ferroelectric phase transition. The authors note that the observed behavior is reminiscent of proper ferroelectrics like  $\text{BaTiO}_3$ , which presents a first-order transition driven by a soft mode with a high permittivity maximum ( $\epsilon_r \approx 10000$ ) associated to it [12]. The authors also assume that the transition connects the o-III and t phases. (A direct transition from o-III to t is supported by some theoretical studies [13] and

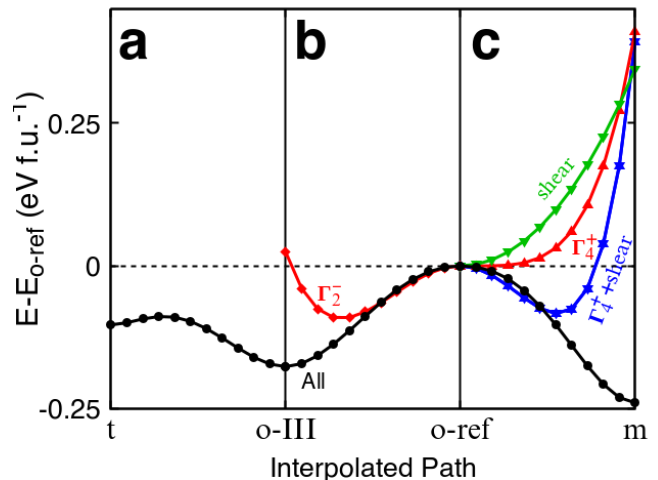


FIG. 2: **Energy landscape connecting key  $\text{HfO}_2$  polymorphs.** The black lines show the computed energy variation between the t and o-III phases (a), o-III and o-ref (b), and o-ref and m (c). The energies are computed for intermediate structures obtained by linear interpolation between the corresponding end-point polymorphs. The red line in b shows the energy variation of the o-ref state upon condensation of the  $\Gamma_2^-$  distortions present in the o-III phase; the red line in c shows the analogous result when considering only the  $\Gamma_4^+$  phonon distortions present in the m-phase. The blue line in c shows the result of condensing together the  $\Gamma_4^+$  phonon and shear strain distortions present in the m-phase, while the green line shows the energy variation associated to the shear alone. In b and c, the additional distortions leading to the black line are fully symmetric  $\Gamma_1^+$  modes, including the normal cell strains.

questioned by others [14].) However, there is a difficulty here: Density Functional Theory (DFT) simulations of  $\text{BaTiO}_3$  show that the paraelectric cubic state presents a dominant polar instability [15, 16], the hallmark of proper ferroelectricity driven by a soft mode. The situation in hafnia is different: according to DFT, the t-phase presents no indication of a polar instability (see Supplementary Figure S1); thus, there is no support for proper soft-mode ferroelectricity. If anything, DFT suggests that a transition between o-III and t would be similar to the ferroelectric-paraelectric transition in  $\text{BiFeO}_3$ : a first-order transformation between two states that DFT describes as local energy minima [17], and which experimentally has a weak dielectric anomaly ( $\epsilon_r \approx 65$ ) associated to it [18, 19].

We now argue that these issues can be resolved by considering a different centrosymmetric reference, namely, the orthorhombic  $Pbcm$  state denoted “o-ref” in Fig. 1b. This structure is similar to o-III, except that the active oxygens (red in the figure) are located within the same plane as the Hf atoms. This o-ref phase has been discussed in theoretical investigations of ferroelectric switching as a potential transition state [20, 21]. As far as we know, there is no experimental evidence for its occur-

rence as a stable polymorph, but that is not an issue for the present purposes. For example, the cubic paraelectric phase of BiFeO<sub>3</sub> is all but inaccessible experimentally [22]; yet, it is the relevant reference to explain the observed ferroelectric domains.

Figure 3a shows the phonon bands computed for the o-ref phase. We find a small number of unstable bands with well-defined character: they feature off-plane displacements of the active oxygens. At the  $\Gamma$  point of the Brillouin zone, there is a dominant instability: a polar mode with symmetry  $\Gamma_2^-$  that captures the distortion connecting o-ref and o-III (Figs. 3b and 3c). Indeed, standard symmetry analysis [23, 24] shows that o-III can be obtained from o-ref by distortions of  $\Gamma_2^-$  and  $\Gamma_1^+$  symmetries, the latter being fully-symmetric modes not relevant in this discussion. The black curve in Fig. 2b shows the energy variation associated to this transformation: a simple potential well with a minimum about 177 meV per formula unit (f.u.) below o-ref. This suggests soft-mode proper ferroelectric behavior as that of BaTiO<sub>3</sub>. Further, the  $\Gamma_2^-$  irreducible representation is one dimensional; thus, we have uniaxial ferroelectricity and no ferroelasticity, as sketched in Fig. 1b and in agreement with experiments.

If we follow the  $\Gamma_2^-$  soft mode along the  $\Gamma - X$  direction of the Brillouin zone, we reach a stronger instability: the antipolar  $X_2^-$  mode in Fig. 3d. This distortion yields another low-energy polymorph: the orthorhombic *Pbca* phase depicted in Fig. 3e, which is usually denoted “o-I” [25] and has been experimentally observed in ZrO<sub>2</sub> [26]. Symmetry analysis shows that o-ref and o-I are connected solely by  $X_2^-$  and fully-symmetric distortions. The o-I state is more favorable than the ferroelectric o-III phase, by about 17 meV per f.u. Further, this state can be seen as an sequence of ultra-thin ferroelectric stripe domains, where the polarization of the o-III phase is modulated along the horizontal direction in Fig. 3b. From this perspective, we can say that the domain walls of the o-III phase have a negative formation energy (of about  $-84 \text{ mJ m}^{-2}$ ) and that ferroelectricity in hafnia is essentially two-dimensional (i.e., a single ultra-thin ferroelectric stripe can occur regardless of its surroundings). This and similar observations (e.g., the slow motion of domain walls in hafnia) had been previously made [27, 28]; here we confirm them from the analysis of the o-ref phase.

Our calculations reveal additional soft modes worth discussing. Especially interesting is the second lowest-lying zone-center instability, with  $\Gamma_4^+$  symmetry and an antipolar character (Fig. 3f). This distortion leads to the well-known monoclinic ground state of hafnia (*P2<sub>1</sub>/c* “m-phase”, Fig. 3g), about 240 meV per f.u. below o-ref [25, 29]. If we follow the  $\Gamma_4^+$  instability as we move towards *X*, we reach a soft mode with symmetry  $X_4^+$ . Sketched in Fig. 3h, this mode involves an antiphase modulation of the antipolar distortion in Fig. 3f; its con-

densation yields the state shown in Fig. 3i, with space group *Pbca* and about 213 meV per f.u. below o-ref, denoted “o-I\*” [25] and experimentally observed [30, 31]. Note that the m and o-I\* phases are both connected to the o-ref state by distortions of well-defined symmetry ( $\Gamma_4^+$  and  $X_4^+$ , respectively) solely accompanied by fully-symmetric modes. Hence, notably, the most relevant low-energy polymorphs of hafnia (m, o-III, o-I and o-I\*) can be obtained as simple proper instabilities of the o-ref phase. Additional low-energy structures – e.g., the “m-III” polar phase recently discussed in Ref. 25 – can be obtained by condensing other soft mode instabilities or combinations of them. Supplementary Figure S2 shows that essentially the same applies to ZrO<sub>2</sub>.

A detailed modeling of the energy landscape of hafnia is beyond the scope of this work. Nevertheless, let us comment on an apparent paradox: given that the computed  $\Gamma_4^+$  phonon instability is weak compared to the others discussed above, how can the associated m-phase be the ground state? To answer this, in Figs. 2b and 2c we distinguish the energy contributions of different sets of modes to stabilize the o-III and m phases. The condensation of the  $\Gamma_2^-$  distortion yields a large energy reduction with respect to o-ref (red curve in Fig. 2b); then, the fully-symmetric  $\Gamma_1^+$  modes react to the ferroelectric distortion and further reduce the energy (black curve) down to the actual o-III minimum. By contrast, the condensation of the  $\Gamma_4^+$  optical distortion alone (red curve in Fig. 2c) yields a shallow energy well. Nevertheless, in the case of the m-phase, the shear strain causing the monoclinic deformation of the cell shares the  $\Gamma_4^+$  symmetry. Hence, while stable by itself (green curve), this shear couples harmonically with the  $\Gamma_4^+$  phonon yielding a much stronger instability (blue curve). In addition, the  $\Gamma_1^+$  modes react to the monoclinic distortion, resulting in the very stable m-phase (black curve). Hence, by using the o-ref phase as the starting point of our analysis, we reveal the key role of the shear strain in determining the ground state of hafnia, reflected in the energetics of Fig. 2c and the fact that the total  $\Gamma_4^+$  instability has a mixed strain-phonon character.

Our approach also sheds light into the possible transitions between stable hafnia polymorphs. For example, an electric field-driven transformation from o-I to o-III constitutes a textbook case of antiferroelectric behavior. Indeed, because the antipolar ( $X_2^-$ ) and polar ( $\Gamma_2^-$ ) instabilities belong to the same band (Fig. 3a), this appears to be an ideal “Kittel antiferroelectric” [32]. Further, we suggest that field-driven transformations from o-I\* to o-III, or from m to o-III, can also be viewed as Kittel-like antiferroelectric transitions, since the polar and antipolar states have a common origin as distortions of the o-ref phase. The latter (m to o-III) would be a rare example of antiferroelectric effect involving no doubling of the unit cell.

Our results also suggest that o-I\* is structurally con-

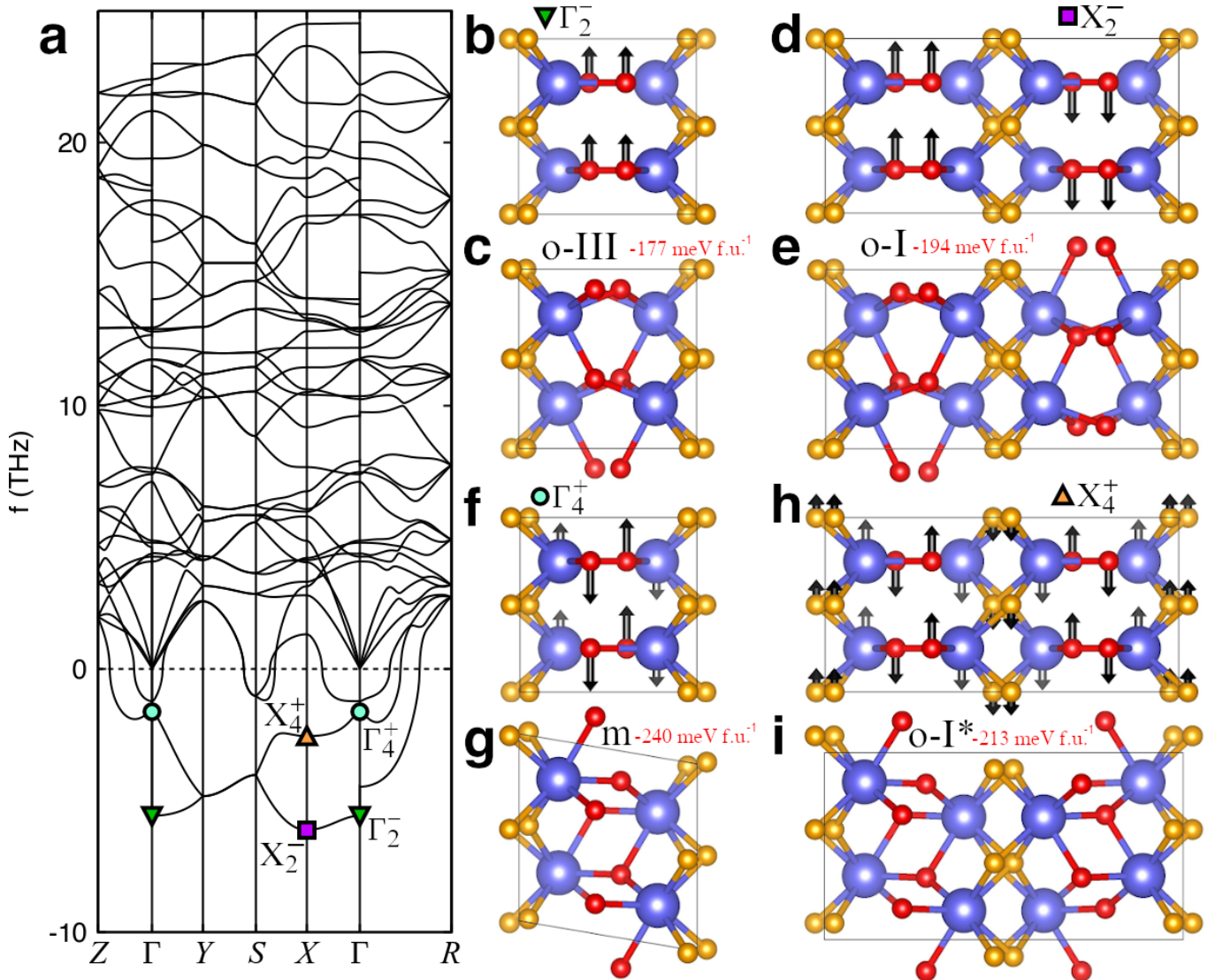


FIG. 3: **Phonon bands of the o-ref phase.** **a** shows the computed bands, presenting imaginary frequencies as negative values. The most important unstable modes are marked in **a**. We also show the corresponding eigenmodes and the polymorphs they lead to: the  $\Gamma_2^-$  soft mode (**b**) and the corresponding o-III phase (**c**); the  $X_2^-$  soft mode (**d**) and the corresponding o-I phase (**e**); the  $\Gamma_4^+$  soft mode (**f**) and the associated m-phase (**g**); and the  $X_4^+$  soft mode (**h**) and the corresponding o-I\* phase (**i**). We mark in red the active oxygens whose displacements characterize these phonons. For the polymorphs, we indicate the energy with respect to o-ref.

nected to the monoclinic ground state. In essence, this connection was already mentioned by Ohtaka *et al* [30]; our theory confirms it and reveals its deeper origin. Indeed, viewed as a distortion of o-ref, the m-phase can present the two variants shown in Fig. 4a, with positive and negative shear, respectively. Then, as emphasized in Fig. 4b, the o-I\* unit cell can be seen as composed of two matching domains corresponding to such m-variants. This is most natural: the underlying  $\Gamma_4^+$  and  $X_4^+$  instabilities belong to the same band, which suggests that the associated distortions correspond to different modulations of the same local motif. Such common motif is the particular antipolar displacement of the active oxy-

gens in Fig. 3f, which is accompanied by a relative vertical shift of the neighboring Hf planes. When this pattern repeats homogeneously ( $\Gamma_4^+$ ) it yields a net shear; when antimodulated ( $X_4^+$ ) the opposing local strains cancel out. These observations further suggest that a transition from o-I\* to m, driven by an appropriate shear stress, would be an example of “antiferroelastic” behavior. Interestingly, antiferroelastics were introduced theoretically decades ago [33], but we are not aware of any demonstration. (The term “antiferroelastic” has been used to denote phases that present correlated antiferrodistortive and Jahn-Teller distortions [34]; however, as far as we can see, such phases do not involve the an-

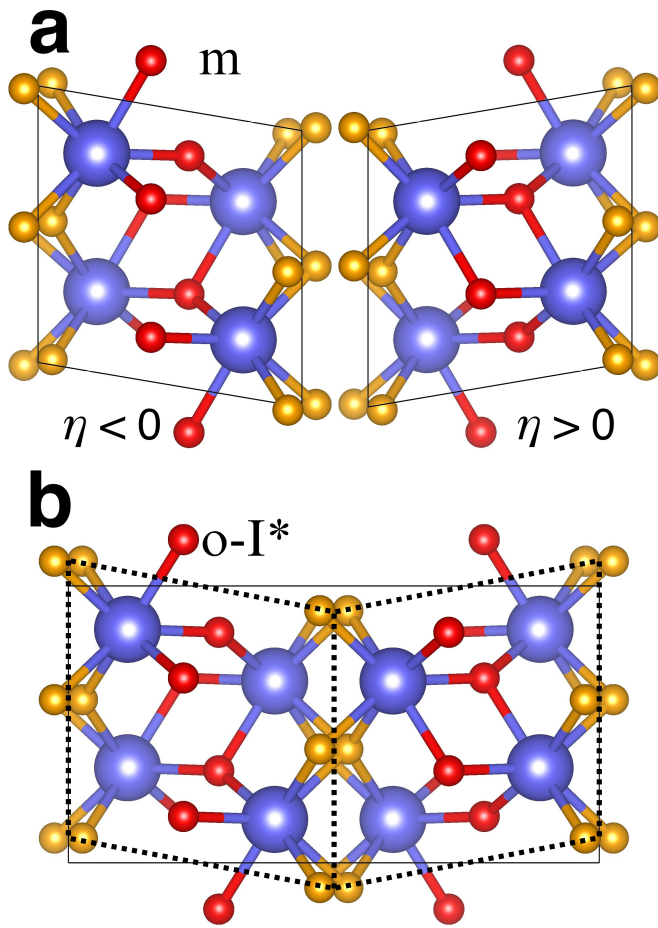


FIG. 4: **Antiferroelastic behavior.** **a** shows the two symmetry-equivalent m-phase variants that can be obtained as a  $\Gamma_4^+$  distortion of the o-ref phase. In **b** we emphasize that the unit cell of the o-I\* phase can be obtained by matching the two m-variants in **a**. Hence, o-I\* can be seen as composed of ultra-thin ferroelastic stripe domains, with a domain wall energy of  $126 \text{ mJ m}^{-2}$ .

tiphas strain modulations discussed by Aizu [33] and shown here.) In the case of hafnia, an experimental realization would require stabilizing the o-I\* state over the m-phase; given their proximity in energy (the gap is about  $27 \text{ meV}$  per f.u.) this is conceivable, e.g., by growing samples on appropriate substrates.

We conclude with some remarks that put our work into perspective. First, note that Zhou *et al.* [14] have recently used DFT to predict that, under suitable elastic constraints, the t-phase evolves into an antipolar state where proper ferroelectric order is eventually triggered. This picture is in principle compatible with the strong dielectric anomaly of Ref. 11, and appears as a viable and complementary alternative to the approach proposed here.

Let us also stress that our work does not explain all of hafnia’s striking behaviors. For example, the states marked with an asterisk in Figs. 1a and 1b are the same;

then, is the polarization of such a structure positive or negative? (See Supplementary Note 1 for a discussion based on the Berry-phase theory [35].) To answer this, in practice we would need to determine which state is reached when we saturate the polarization by application of a positive electric field: the state marked with an asterisk in Fig. 1a, or that marked with a dagger in Fig. 1b? In turn, this will depend on the details of ferroelectric switching [21]: is it realistic to assume that it proceeds through the t-phase, so that a positive field yields the state marked with an asterisk in Fig. 1a? Or does it go through o-ref, so we reach the state marked with a dagger in Fig. 1b? Similar issues affect the question of the sign of the piezoelectric response of hafnia [4, 21], which ultimately depends on which is the state with positive polarization. None of these problems are resolved here.

Another issue beyond the scope of the present treatment is that of the (kinetic) mechanisms to stabilize or wake up the o-III ferroelectric phase [36]. Nevertheless, our observations suggest that – since they are related to a specific o-ref state – the presence of m, o-I or o-I\* polymorphs in the samples may contribute to breaking the tetragonal (or cubic) symmetry and determine the polarization easy axis, which would result in the observed uniaxial ferroelectricity.

Our treatment is thus limited to the thermodynamic and response properties of the most frequently observed ferroelectric phase of hafnia-related materials, potentially including field- and temperature-driven transitions, but probably insufficient to tackle other important aspects (kinetic origin, ferroelectric switching). Within that restricted – but crucial – realm, our work provides a simple yet thorough picture of the relevant energy landscape, naturally connecting all low-energy polymorphs, and describing hafnia as a uniaxial proper ferroelectric that is not ferroelastic. Remarkably, the proposed reference phase appears as an ideal starting point for the development of physically transparent perturbative theories, from phenomenological Ginzburg-Landau models to coarse-grained effective Hamiltonians [37] or atomistic second-principles potentials [38]. Further, having a model of hafnia as a soft-mode ferroelectric invites (enables) us to borrow ideas from the literature on perovskite oxides, for example, to optimize the negative capacitance effect [39, 40]. We thus expect our findings will become an important ingredient of future work on these materials, from theoretical and computational studies to the conception of new experiments and optimization strategies.

**Methods.** Our simulations are carried out using first-principles density functional theory (DFT) as implemented in the Vienna Ab-initio Simulation Package (VASP) [41, 42]. We employ the Perdew-Burke-Ernzerhof formulation for solids (PBEsol) [43] of the generalized gradient approximation for the exchange-correlation functional. The atomic cores are treated

within the projector-augmented wave approach [44], considering the following states explicitly: 5s, 5p, 6s, 5d for Hf; 4s, 4p, 5s, 4d for Zr; and 2s, 2p for O. We use a plane-wave energy cutoff of 600 eV. A  $6 \times 6 \times 6$  Monkhorst-Pack [45]  $k$ -point sampling of the Brillouin zone is employed for the o-ref, m, t and o-III phases, and a  $3 \times 6 \times 6$   $k$ -point grid is employed for the o-I and o-II phases, which are (approximately) twice as long along the first lattice vector. The structures are fully relaxed until the residual forces fall below  $0.001 \text{ eV \AA}^{-1}$  and residual stresses fall below 0.01 GPa. These calculation conditions yield well-converged results.

The paths shown in Fig. 2 are obtained by interpolating the lattice vectors and fractional atomic coordinates between the initial and final structures with 10 intermediate points. No structural optimization is performed for the intermediate states. The polarization is computed using the modern theory of polarization [35].

Phonon bands are obtained using the direct supercell approach implemented in the PHONOPY package [46]. A  $2 \times 2 \times 2$  supercell is employed both for the o-ref phase of  $\text{HfO}_2$  and  $\text{ZrO}_2$  and for the t-phase of  $\text{HfO}_2$ , which we find to give well-converged results. The non-analytical contribution to the phonons is considered in the calculations.

We use standard web-based crystallographic tools [23, 24] for symmetry analysis. The visualization package VESTA [47] is used for the structure representations.

**Acknowledgments.** Work supported by the Luxembourg National Research Fund through Grant INTER/NWO/20/15079143/TRICOLOR.

- 
- [1] T. S. Böscke, J. Müller, D. Bräuhäus, U. Schröder, and U. Böttger, *Applied Physics Letters* **99**, 102903 (2011).
- [2] J. Müller, T. S. Böscke, U. Schröder, S. Mueller, D. Bräuhäus, U. Böttger, L. Frey, and T. Mikolajick, *Nano Letters* **12**, 4318 (2012).
- [3] M. T. Bohr, R. S. Chau, T. Ghani, and K. Mistry, *IEEE Spectrum* **44**, 29 (2007).
- [4] S. Dutta, P. Buragohain, S. Glinsek, C. Richter, H. Aramberri, H. Lu, U. Schroeder, E. Defay, A. Gruverman, and J. Íñiguez, *Nature Communications* **12**, 7301 (2021).
- [5] S. E. Reyes-Lillo, K. F. Garrity, and K. M. Rabe, *Physical Review B* **90**, 140103 (2014).
- [6] F. Delodovici, P. Barone, and S. Picozzi, *Phys. Rev. Mater.* **5**, 064405 (2021).
- [7] P. Zhou, B. Zeng, W. Yang, J. Liao, F. Meng, Q. Zhang, L. Gu, S. Zheng, M. Liao, and Y. Zhou, *Acta Materialia* **232**, 117920 (2022).
- [8] R. S. Weis and T. K. Gaylord, *Applied Physics A* **37**, 191 (1985).
- [9] G. Catalan and J. F. Scott, *Advanced Materials* **21**, 2463 (2009).
- [10] D. A. Scrymgeour, V. Gopalan, A. Itagi, A. Saxena, and P. J. Swart, *Phys. Rev. B* **71**, 184110 (2005).
- [11] U. Schroeder, T. Mittmann, M. Materano, P. D. Lomenzo, P. Edgington, Y. H. Lee, M. Alotaibi, A. R. West, T. Mikolajick, A. Kersch, et al., *Advanced Electronic Materials* **8**, 2200265 (2022).
- [12] F. Jona and G. Shirane, *Ferroelectric crystals* (Dover Publications, 1993), ISBN 0486673863.
- [13] J. Liu, S. Liu, L. H. Liu, B. Hanrahan, and S. T. Pantelides, *Phys. Rev. Appl.* **12**, 034032 (2019).
- [14] S. Zhou, J. Zhang, and A. M. Rappe, *Science Advances* **8**, eadd5953 (2022).
- [15] R. D. King-Smith and D. Vanderbilt, *Physical Review B* **49**, 5828 (1994).
- [16] P. Ghosez, E. Cockayne, U. V. Waghmare, and K. M. Rabe, *Physical Review B* **60**, 836 (1999).
- [17] O. Diéguez, O. E. González-Vázquez, J. C. Wojdeł, and J. Íñiguez, *Physical Review B* **83**, 094105 (2011).
- [18] M. Polomska, W. Kaczmarek, and Z. Pajak, *Physica Status Solidi (a)* **23**, 567 (1974).
- [19] D. C. Arnold, K. S. Knight, F. D. Morrison, and P. Lightfoot, *Phys. Rev. Lett.* **102**, 027602 (2009).
- [20] S. Clima, D. J. Wouters, C. Adelmann, T. Schenk, U. Schroeder, M. Jurczak, and G. Pourtois, *Applied Physics Letters* **104**, 092906 (2014).
- [21] Y. Qi, S. E. Reyes-Lillo, and K. M. Rabe, <https://arxiv.org/abs/2204.06999> (2022).
- [22] D. C. Arnold, K. S. Knight, G. Catalan, S. A. T. Redfern, J. F. Scott, P. Lightfoot, and F. D. Morrison, *Advanced Functional Materials* **20**, 2116 (2010).
- [23] B. J. Campbell, H. T. Stokes, D. E. Tanner, and D. M. Hatch, *Journal of Applied Crystallography* **39**, 607 (2006).
- [24] M. I. Aroyo, J. M. Perez-Mato, C. Capillas, E. Kroumova, S. Ivantchev, G. Madariaga, A. Kirov, and H. Wondratschek, *Zeitschrift für Kristallographie* **221**, 15 (2006).
- [25] L. Azevedo Antunes, R. Ganser, C. Kuenneth, and A. Kersch, *physica status solidi (RRL) – Rapid Research Letters* **16**, 2100636 (2022).
- [26] O. Ohtaka, T. Yamanaka, S. Kume, N. Hara, H. Asano, and F. Izumi, *Proceedings of the Japan Academy, Series B* **66**, 193 (1990).
- [27] H.-J. Lee, M. Lee, K. Lee, J. Jo, H. Yang, Y. Kim, S. C. Chae, U. Waghmare, and J. H. Lee, *Science* **369**, 1343 (2020).
- [28] Y. Qi, S. Singh, and K. M. Rabe, <https://arxiv.org/abs/2108.12538> (2021).
- [29] S. Barabash, *Journal of Computational Electronics* **16**, 1227 (2017).
- [30] O. Ohtaka, T. Yamanaka, S. Kume, N. Hara, H. Asano, and F. Izumi, *Journal of the American Ceramic Society* **78**, 233 (1995).
- [31] H. Du, C. Groh, C.-L. Jia, T. Ohlerth, R. E. Dunin-Borkowski, U. Simon, and J. Mayer, *Matter* **4**, 986 (2021).
- [32] C. Kittel, *Phys. Rev.* **82**, 729 (1951).
- [33] K. Aizu, *Journal of the Physical Society of Japan* **27**, 1171 (1969).
- [34] S. Watanabe, M. Hidaka, H. Yoshizawa, and B. M. Wanklyn, *Physica Status Solidi (b)* **243**, 424 (2006).
- [35] R. D. King-Smith and D. Vanderbilt, *Physical Review B* **47**, 1651 (1993).
- [36] M. H. Park, Y. H. Lee, T. Mikolajick, U. Schroeder, and C. S. Hwang, *Advanced Electronic Materials* **5**, 1800522 (2018).

- [37] W. Zhong, D. Vanderbilt, and K. M. Rabe, *Physical Review Letters* **73**, 1861 (1994).
- [38] J. C. Wojdeł, P. Hermet, M. P. Ljungberg, P. Ghosez, and J. Íñiguez, *Journal of Physics: Condensed Matter* **25**, 305401 (2013).
- [39] J. Íñiguez, P. Zubko, I. Luk'yanchuk, and A. Cano, *Nature Reviews Materials* **4**, 243 (2019).
- [40] M. Graf, H. Aramberri, P. Zubko, and J. Íñiguez, *Nature Materials* **21**, 1252 (2022).
- [41] G. Kresse and J. Furthmüller, *Physical Review B* **54**, 11169 (1996).
- [42] G. Kresse and D. Joubert, *Physical Review B* **59**, 1758 (1999).
- [43] J. Perdew, A. Ruzsinszky, G. Csonka, O. Vydrov, G. Scuseria, L. Constantin, X. Zhou, and K. Burke, *Physical Review Letters* **100**, 136406 (2008).
- [44] P. E. Blöchl, *Physical Review B* **50**, 17953 (1994).
- [45] H. J. Monkhorst and J. D. Pack, *Physical Review B* **13**, 5188 (1976).
- [46] A. Togo and I. Tanaka, *Scr. Mater.* **108**, 1 (2015).
- [47] K. Momma and F. Izumi, *Journal of Applied Crystallography* **44**, 1272 (2011).